Journal of Physics: Conference
Series

Limitations of the enthalpy-porosity method for numerical simulation of close-contact melting on inclined surfaces

To cite this article: V Van Riet *et al* 2024 *J. Phys.: Conf. Ser.* **2766** 012214

Limitations of the enthalpy-porosity method for numerical simulation of close-contact melting on inclined surfaces

V Van Riet[1,2], T Shockner[3], W Beyne[1,2], G Ziskind[3], M De Paepe[1,2] and J Degroote[1,2]

[1]Ghent University, Sint-Pietersnieuwstraat 41, Ghent, 9000, Belgium
[2]FlandersMake@UGent – Core lab MIRO, Ghent, 9000, Belgium
[3]Ben-Gurion University of the Negev, Beer-Sheva 84105, Israel

Email: Victor.VanRiet@UGent.be

Abstract. One of the main challenges for latent thermal energy storage (LTES) systems is low heat transfer rates due to the low thermal conductivity of most phase change materials (PCM). Close-contact melting (CCM) can accelerate melting times in LTES systems but the current numerical techniques for solid liquid phase change have difficulties with accurately predicting this process. In this study, close-contact melting of PCM on an inclined surface is simulated using the enthalpy-porosity method in ANSYS Fluent. All PCM properties, including density, are temperature-dependent. In this way, phenomena such as natural convection, volume change and buoyancy between the solid and liquid are taken into account. The volume change is compensated by a gaseous expansion volume. Both 2D and 3D simulations are used to show discrepancy between state-of-the-art enthalpy porosity modelling and experimentally observed phenomena in the case of CCM. The mushy zone constant, which is set to 10^5 to allow motion of the solid bulk, causes the solid phase to deform as a highly viscous fluid instead of moving as a rigid body. The velocity differences inside the solid are more than 50 % of its sinking velocity. As a result, the movement of the solid resembles creep behaviour and the obtained CCM patterns are not physically accurate. Furthermore, the density difference between the solid and liquid phases causes an avalanching effect in the mushy zone, which artificially strengthens convection. In conclusion, the enthalpy porosity method exhibits significant limitations in accurately capturing close-contact melting phenomena.

1. Introduction

Latent thermal energy storage (LTES) systems are a promising technology to match the supply of renewable energy and thermal energy demands. A major shortcoming of LTES systems is the low inherent thermal conductivity of most practical phase change materials (PCM) [1]. As a result, charging an LTES system solely based on conduction through the PCM would significantly reduce its application potential and heat transfer augmentation is often required in the design of LTES heat exchangers [2]. Close-contact melting (CCM) is very promising in this regard because it can reduce melting times by a factor of up to 2.5 in practically feasible systems [3].

During close-contact melting, the solid PCM is pressed down on a heated surface either by gravity or by an external force, and a liquid layer is formed and maintained between the solid bulk and the heated surface, which enables high heat transfer rates [4]. The principle of CCM has been investigated in many experimental heat exchanger test setups in recent years [3 - 7]. This study focuses on the triple tube heat exchanger with longitudinal plate fins presented by Shockner et al. in [2]. As stated in their paper, if the heat exchanger is placed in the so-called ‘Mercedes’ configuration, close-contact melting occurs on inclined surfaces in the upper part of the heat exchanger. The fin orientation in the ‘Mercedes’ configuration is shown in figure 1. The geometry is further explained in section 2. For more details on the test setup and experimental results, the reader is referred to [2] and [3].

The goal of this study is to numerically model this melting process using the enthalpy-porosity method. The enthalpy-porosity method, developed by Voller et al. [8], is one of the most commonly used models for solid-liquid phase change because of its availability in commercial CFD packages. The enthalpy-porosity method, however, poses a problem in the choice of the mushy zone constant. The choice of this constant, which is used in the source term of the momentum equation, has a significant influence on the simulated phase change process [9]. In case of close-contact melting, the value of the mushy zone constant is typically chosen low (e.g. 10^5) because higher values (up to 10^8) would completely supress any velocity of the solid phase. A low mushy zone constant, on the other hand, allows movement of the solid bulk [10]. This movement, however, shows more resemblance to creep in a highly viscous fluid, than to motion of a rigid body. Despite these issues, many studies apply the enthalpy-porosity method for numerical modelling of close-contact melting problems, e.g. [11 - 13], with mushy zone constants as low as $2 \cdot 10^4$ [13]. In these studies, the authors mention similar problems with the enthalpy-porosity method.

Section 2 presents the numerical methods used in this study. The simulations use temperature-dependent material properties. This induces natural convection in the melt and volume change during phase change, which is compensated by an expansion volume filled with air. Despite these efforts, the inherent limitations of the enthalpy-porosity method are apparent. Besides the creeping behaviour, the results also show artificial convection in the mushy zone. The results are discussed in section 3.

2. Numerical methods

2.1. Geometry and mesh

The geometry is based on the triplex tube heat exchanger introduced in [2], oriented in the ‘Mercedes’ configuration. Figure 1 shows a cross-sectional view of the heat exchanger with longitudinal plate fins that divide the storage space for the PCM in three parts. The dimensions of the simulated domain are based on the test device, which is also presented in [2] and shown in figure 2.

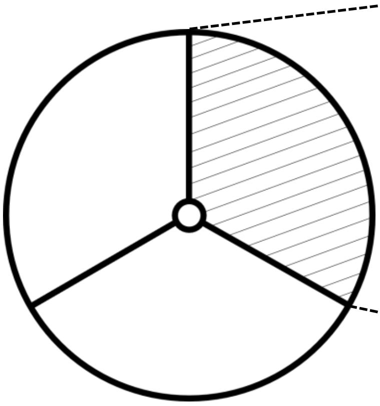

Figure 1. Cross-sectional view of the triplex tube heat exchanger (simulated part marked).

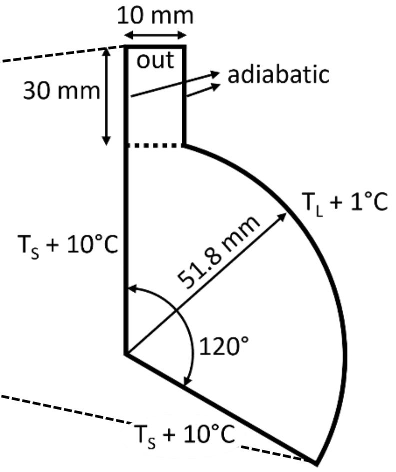

Figure 2. Geometry of the simulated domain with dimensions, thermal boundary conditions and outlet on top indicated.

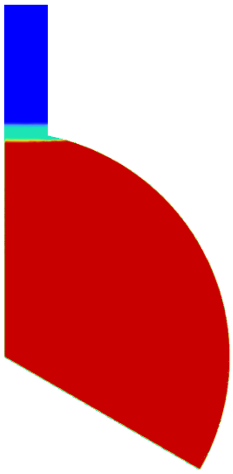

Figure 3. Initial conditions in the 2D and 3D domain: air (blue), liquid PCM (green) and solid PCM (red).

This test device in [2] represents the enlarged upper 1/3 of the heat exchanger in [3], which is marked in the cross-sectional view of figure 1. The test device has a circular wall with radius of 51.8 mm, which makes an arc of 120°. The domain is closed with a vertical and downward inclined heated wall. At the top, an expansion volume is included, with a width of 10 mm and a height of 30 mm, to buffer the expansion of the PCM during melting. The test device on which the domain is based has a depth (perpendicular to the plane of the figure) of 28 mm and is bound on front and back by transparent Perspex plates [2]. The inclined surface causes the solid bulk to both translate and rotate during melting.

Two simulations are performed: in 2D and 3D. The 2D computational domain has the dimensions as described above and as shown in figure 2. The 3D domain has identical in-plane dimensions as the 2D domain but is extruded in the third dimension with a depth of 14 mm. This is half the depth of the test device because symmetry is assumed at the mid-plane between the two Perspex plates.

The 2D domain is meshed in an unstructured way and has 20795 cells with a standard cell sizing of 0.446 mm. This value is chosen to match the cell height of the last cell in the inflation layers at the two heated walls, the circular wall and the left wall of the expansion volume. The inflation layers have a thickness of 13 cells, a growth rate of 1.2 and a cell thickness for the first layer of 0.05 mm. The 3D domain is also meshed in an unstructured way and has 455301 cells with a standard cell sizing of 0.5 mm. The inflation layers are adaptively generated with a thickness of 13 layers and a growth rate of 1.2. The inflation layers are applied to the two heated walls, the circular wall and the front wall (not the symmetry plane). Consequently, the expansion volume has no inflation layers in the 3D domain.

2.2. Boundary and initial conditions

Figure 3 shows the initial conditions in both the 2D and 3D domain. The expansion volume is filled with air at 315 K and the rest of the domain is filled with PCM. To avoid numerical instabilities, there is a small layer of liquid PCM at 315 K between the air and solid PCM, which is at 309.85 K, its solidus temperature T_S. All phases have zero velocity initially.

Figure 2 shows the boundary conditions in the 2D domain. The domain has no inlet and a single pressure outlet boundary condition for air at the top of the expansion volume. The other edges are walls with a no-slip boundary condition. The thermal boundary conditions consist of adiabatic walls in the expansion volume and constant temperature boundary conditions on the other walls. The two heated walls are 10 K above solidus temperature (319.85 K) and the circular wall is 1 K above liquidus temperature T_L (311.35 K), to avoid the solid bulk remaining attached to this wall.

In the 3D domain, the back has a symmetry boundary condition, and the front has a no-slip boundary condition with a temperature of 1 K above T_L as well, to enable solid bulk motion.

2.3. Material properties

The PCM properties are based on eicosane ($C_{20}H_{42}$) because this was used in the experiments of [2]. Pure eicosane has a melting point of 36.7 °C (309.85 K). This is set equal to the solidus temperature T_S in the simulation, because enthalpy methods for phase change require a melting range. In this study, a small melting range of 0.5 °C has been chosen, which means the liquidus temperature T_L is equal to 37.2 °C (310.35 K). The full material properties are presented in Table 1 and are based on [4] and [14].

Table 1. Properties of eicosane ($C_{20}H_{42}$) used in the simulations.

	Dynamic viscosity μ (kg/m s)	Sensible specific heat capacity c_p (J/kg K)	Thermal conductivity k (W/m K)	Density ρ (kg/m³)	Latent heat L (kJ/kg)
Solid	/	1926	0.4	856	248
Liquid	0.00401 @ 309.85 K	2400	0.15	775.13 @ 309.95 K	
	0.00320 @ 323.20 K			768.33 @ 323.15 K	
	0.00261 @ 333.20 K			761.72 @ 333.15 K	
	0.00217 @ 343.20 K			755.07 @ 343.15 K	

The air is modelled with a constant specific heat equal to 1006.43 J/kg K, a thermal conductivity of 0.0242 W/m K, a viscosity of $1.7894 \cdot 10^{-5}$ kg/m s and a temperature dependent density (kg/m³): $\rho = 1.2 \cdot 10^{-5} T^2 - 0.01134 T + 3.4978$ [9].

2.4. Governing equations

The volume-of-fluid (VOF) method is used to solve the governing equations with two media present in the computational domain: air and PCM. The volume fraction of the ith fluid in a cell is denoted as α_i and its value should always be between 0 and 1, with 1 indicating that the cell is completely filled with that fluid. Using the material derivative notation, the governing equations can be written as [9]:

- Volume fraction equation: $$\frac{D\alpha_i}{Dt} = 0 \tag{1}$$
- Momentum equation: $$\frac{\rho D\vec{v}}{Dt} = -\nabla p + \mu\nabla^2\vec{v} + \rho\vec{g} + \vec{S} \tag{2}$$
- Energy equation: $$\frac{\rho DH}{Dt} = k\nabla^2 T \tag{3}$$

where ρ is the density, μ the dynamic viscosity and k the thermal conductivity of the fluid present in the cell. In case of a mixture, in the cells at the air-PCM interface, the values of the properties are an average weighed by the volume fraction values. Furthermore, $\vec{v}$ is the velocity vector, p the pressure field, T the temperature and H the sum of the sensible enthalpy h and the enthalpy change due to phase change γL, with L the latent heat of the PCM and γ the liquid fraction defined as follows [8]:

$$\gamma = \begin{cases} 0 & if\ T < T_S \\ 1 & if\ T > T_L \\ \frac{T-T_S}{T_L-T_S} & if\ T_S < T < T_L \end{cases} \tag{4}$$

The source term in the momentum equation $\vec{S}$ forces the velocity to zero as the liquid fraction γ tends to zero in the mushy zone. The source term is defined as [8]:

$$\vec{S} = \frac{(1-\gamma)^2}{(\gamma^3+\varepsilon)} A_{mush}\vec{v} \tag{5}$$

with ε a small number (0.001) to avoid division by zero and A_{mush} the mushy zone constant, which is set to 10^5 in this study to allow limited motion in the solid bulk.

The equations were solved numerically with a SIMPLE pressure-velocity coupling algorithm. The gradients were computed with a least squares cell based method, and the pressure interpolation scheme was PRESTO!. The momentum and energy equations were discretised with the first-order scheme, the VOF interface is captured by the Geo-Reconstruct scheme and the bounded second-order implicit formulation was chosen for the time-stepping with a fixed time step size of 0.01 s.

3. Results and discussion

The enthalpy-porosity method was used as implemented in the CFD package ANSYS Fluent 2023R1 and a grid convergence study was performed to assure grid independent results.

3.1. 2D simulation

Figure 4 shows the contour of liquid fraction at three different time instances. The evolution of liquid fraction in time is presented in figure 7. A clear sinking motion of the solid bulk can be observed. This is achieved by setting A_{mush} to a low (though very popular in the literature) value of 10^5. Despite this, CCM can not be reliably simulated because the thickness of the liquid layer grows significantly over time in these simulations, which is unphysical.

Figure 5 reveals the true behaviour of the solid bulk motion. The velocity vectors inside the solid PCM show a wide spread in their velocity magnitude. The velocity ranges from $5.5 \cdot 10^{-6}$ m/s to $8.5 \cdot 10^{-6}$ m/s, which is a 55 % difference, and the vectors do not look physically meaningful. This indicates that the solid phase does not behave as a rigid body, as it should, but as a highly viscous fluid. Consequently, the observed solid bulk motion does not represent the expected rigid body motion but resembles creeping behaviour.

Figure 6 reveals another defect of the enthalpy-porosity method. At the solid-liquid interface, high liquid velocities can be observed. These are not physically accurate but result from the strong density change during phase change in the mushy zone. As the liquid fraction decreases in the thin mushy zone, the density of the PCM increases by 10.4 %. In case of a small mushy zone constant, needed to enable motion in the solid phase, the velocities in the mushy zone are not sufficiently reduced to avoid a strong artificial convection current. This effect, which may be called 'avalanching', artificially increases the melting rate and compensates the reduced heat transfer due to the inability to simulate CCM.

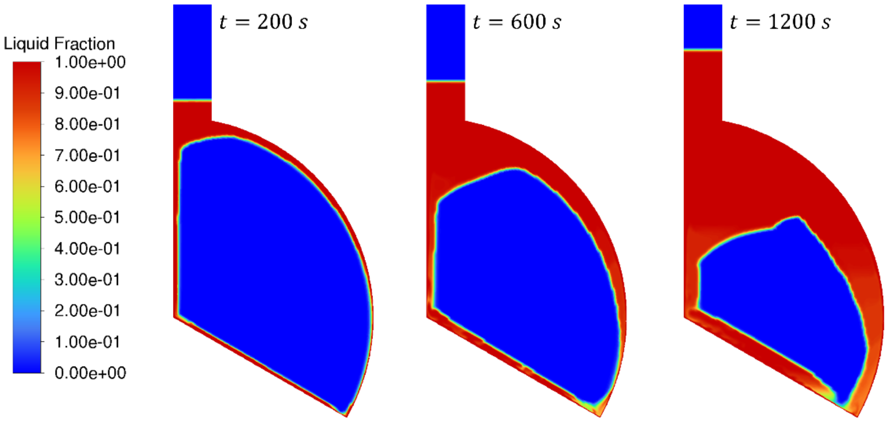

Figure 4. Contour of liquid fraction at 200 s, 600 s and 1200 s (red = liquid PCM, top blue = air and bottom blue = solid PCM) in 2D

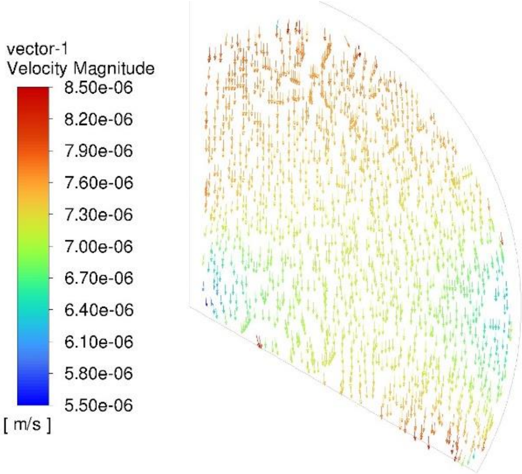

Figure 5. Velocity vectors in the solid PCM at 270 s (coloured by velocity magnitude) in 2D

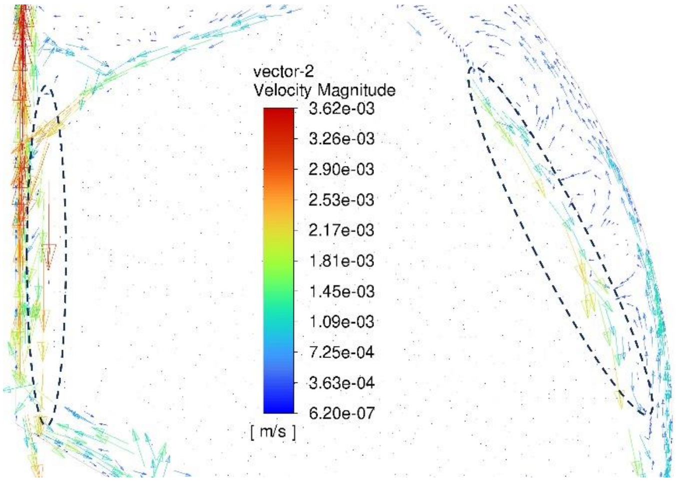

Figure 6. Velocity vectors in the liquid melt at 840 s (coloured by velocity magnitude) in 2D

3.2. 3D simulation

The 3D simulation revealed the same melting behaviour and deficiencies of the enthalpy-porosity method. Yet, the melting rate is much higher, as observed in figure 7. This follows from the observation in figure 8 that much stronger melting occurs near the Perspex panels than expected. Figure 8 displays the contour of the liquid fraction in a cross-sectional plane passing through the centre of the circle section, tilted 30 degrees from the horizontal. The higher melting rate can be attributed, again, to the artificial avalanching effect on the large solid-liquid interface at the front panel.

4. Conclusions

This study applied the enthalpy-porosity method to simulate melting behaviour in an experimental test device inspired by a triplex tube heat exchanger. The downward inclined heated surface enabled close-contact melting. As a result, the motion of the solid PCM was non-trivial, with both translation and rotation of the solid body. Solid body motion was achieved by choosing a small mushy zone constant. The enthalpy-porosity method, however, was unable to maintain the thin liquid layer as the solid phase shrunk over time, which disabled the mechanism of close-contact melting. Additionally, the solid bulk motion exhibited features of highly viscous fluid flow and artificial convection currents. These limitations highlight the need for caution when employing the enthalpy-porosity method for solid-liquid phase change simulations.

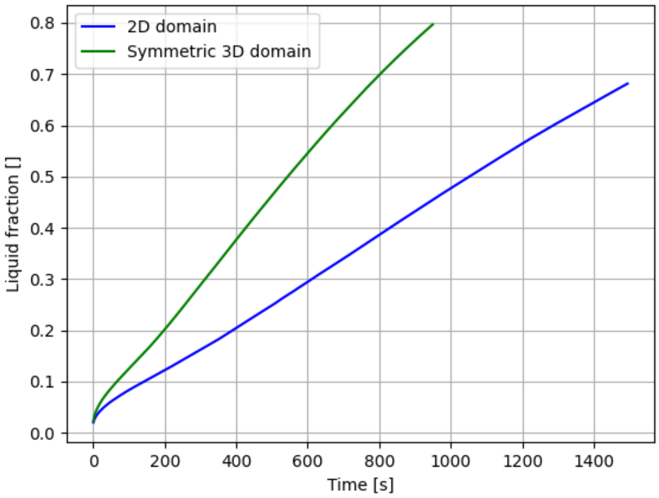

Figure 7. Liquid fraction as a function of time for the 2D and 3D simulation

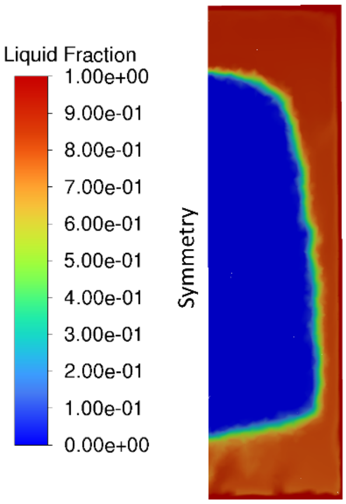

Figure 8. Contour of liquid fraction in the plane 30° above the horizontal.

Acknowledgements

This work was supported by the Special Research Fund (BOF) at Ghent University [BOF22/DOC/076] and by the Research Foundation – Flanders (FWO) [travel grant V427323N] & [grant 1246924N].

References

[1] Ziskind G, Kozak Y 2018 *Encyclopedia of Thermal Packaging* vol 3, ed A Bar-Cohen (Maryland: World Scientific) pp 1–270
[2] Shockner T, Salman I, Greenwald I, Portnikov D, Ziskind G 2023 *Proc. 17th Int. Heat Transfer Conf.*
[3] Rozenfeld T, Kozak Y, Hayat R, Ziskind G 2015 *Int J Heat Mass Transf* **86** 465–77
[4] Kozak Y, Rozenfeld T, Ziskind G 2014 *Int J Heat Mass Transf* **72** 114–27
[5] Fu W, Yan X, Gurumukhi Y, Garimella VS, King WP, Miljkovic N 2022 *Nature Energy* **7** 270–80
[6] Rozenfeld A, Kozak Y, Rozenfeld T, Ziskind G 2017 *Int J Heat Mass Transf* **110** 692–709
[7] Kasibhatla RR, Brüggemann D 2021 *Appl Therm Eng* **184** 116301
[8] Voller VR, Prakash C 1987 *Int J Heat Mass Transf* **30** 1709–19
[9] Shmueli H, Ziskind G, Letan R 2010 *Int J Heat Mass Transf* **53** 4082–91
[10] Kozak Y, Ziskind G 2017 *Int J Heat Mass Transf* **112** 568–86
[11] Assis E, Katsman L, Ziskind G, Letan R 2007 *Int J Heat Mass Transf* **50** 1790–804
[12] Pan C, Charles J, Vermaak N, Romero C, Neti S, Zheng Y, et al. 2018 *Int J Heat Mass Transf* **124** 1015–24
[13] Baghaei Oskouei S, Li ZR, Bayer Ö, Fan LW 2024 *Int J Heat Mass Transf* **218** 124795
[14] Queimada AJ, Marrucho IM, Coutinho JAP, Stenby EH 2005 *Int J Thermophys* **26** 47–61